9th Int.Symp. "Nanostructures: Physics and Technology" NT.24p
St Petersburg, Russia, June 18-22, 2001

Nitrogen-activated phase separation in InGaAsN/GaAs heterostructures grown by MBE

I. P. Soshnikov[1], N. N. Ledentsov[1], B. V. Volovik[1], A. Kovsh[1], N. A. Maleev[1], S. S. Mikhrin[1], O. M. Gorbenko[6], W. Passenberg[2], H. Kuenzel[2], N. Grote[2], V. M. Ustinov[1], H. Kirmse[3], W. Neuman[3], P. Werner[4], N. D. Zakharov[4], D. Bimberg[5] and Zh. I. Alferov[1]

[1] Ioffe Physico-Technical Institute, St Petersburg, Russia
[2] Heinrich-Hertz-Institut für Nachrichtentechnik, Berlin, Germany,
[3] Humboldt Universität Berlin, Insitut für Physik, 10115 Berlin, Germany
[4] Max-Plank-Institut für Mikrostrkturphysik, 06120 Halle, Germany
[5] Institut für Festkörperphysik, TU Berlin, 10623 Berlin, Germany
[6] Institute for Analytical Instrumentation, St Petersburg, 198103 Russia

Abstract. InGaAsN insertions in a GaAs matrix grown by molecular beam epitaxy (MBE) demonstrate a pronounced effect of phase separation even at relatively low indium and nitrogen concentrations. Cross-section high-resolution transmission electron microscopy (TEM) images, processed using a specially-developed software, demonstrated an effect of nitrogen decoration of InAs-rich regions in the structures studied. Formation of ordered structures of compositional domains has been revealed in plan-view TEM images.

Introduction

We report on studies of InGaAsN insertions in a GaAs matrix using transmission electron microscopy (TEM), high-resolution TEM (HRTEM) and HRTEM image processing. InGaAsN-based structures recently attracted much attention due to the possibility to cover the long wavelength spectral range (1.3 and 1.55 μm) using GaAs substrates [1]. Several groups have reported on the fabrication of InGaAsN/GaAs based devices using molecular beam epitaxy (MBE) [2–7] or MOCVD [8, 9] growth techniques. At the same time the main growth mechanisms and the internal structure of these insertions is still not well understood.

Experimental

In this work we study 6 nm-thick InGaAsN insertions in a GaAs matrix grown by MBE using RIBER 32 machine with RF nitrogen source on (100)-oriented GaAs substrates.

We used a special pneumatic separator between the vacuum chamber and the nitrogen source. This allowed us to control plasma-assisted epitaxy on a very short time scale (around 1 s), which is much shorter than the transient processes in the RF plasma itself. Changing the power of the RF plasma source varied nitrogen content. RHEED was used for in situ characterization of the surface morphology. The samples' descriptions are listed in Table 1.

Table Nominal parameters of the structures studied.

		Power of	Size of the		PL peak
Sample	In-content	the nitrogen	lateral	RHEED	energy (eV)
1	0.25	0	Not observed	streaky	1.214
2	0.25	75 W	Not observed	streaky	1.130
3	0.25	160 W	~35 nm	dashed	1.020
4	0.30	75 W	~30 nm	dashed	1.133
5	0.30	115 W	~25 nm	spotty	1.068
6	0.35	0	—	spotty	—
7	0.35	75 W	~25 nm	spotty	1.06
8	0.40	75 W	~30 nm	spotty	1.080

Specimens for TEM study were prepared by standard methods using 4 keV Ar^+ ion beam etching. HREM images were processed using the image-processing technique [10] based on the evaluation of the local lattice parameter. Photoluminescence was excited using a 514.5 nm line of Ar^+ laser at 300 K and detected with a cooled Ge photodiode.

Results and discussion

The results of TEM studies indicate that the samples can be roughly divided in two main groups. The samples with low indium (x~ 0.25) and/or nitrogen (y~75 W or less) contents emitting at and below 1 μm at room temperature demonstrate layer-like contrast in TEM with uniform interfaces. HRTEM image of such a structure is shown in Fig. 1(a). The image processing of the HREM image (Fig. 1(b)) shows nevertheless the modulations of the local interplane distance a_{200}, which is defined by an expression

$$-0.03 \leq \delta\, a_{InGaAsN}/a_{GaAs} \leq 0.05 \qquad (1)$$

where $\delta\, a_{InGaAsN} = a_{InGaAsN} - a_{GaAs}$ is different of local interplane distances of InGaAsN and of matrix.

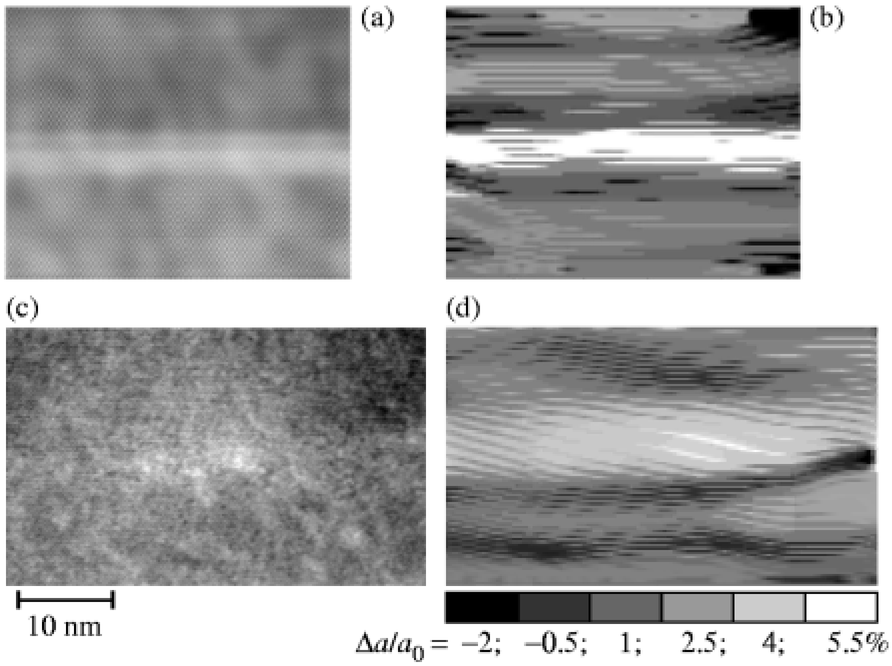

Fig 1. HREM images of $In_{0.25}Ga_{0.75}As_{0.994}N_{0.006}$/GaAs (a) and $In_{0.30}Ga_{0.70}As_{0.99}N_{0.01}$/GaAs (b) insertions and their tone-coded maps of local interplane distance in vertical direction (c, d, respectively).

The range of values of the local lattice parameter fits to the whole range of the lattice parameters of the InAs-GaAs system, pointing to severe InAs local accumulation effect also in the case of planar layers ($-0.005 \leq \delta\, a_{InGaAsN}/a_{GaAs} \leq 0.08$). Even more interesting, negative negative values of $\delta\, a_{InGaAsN}$ are found, as opposite to the InGaAs-GaAs quantum well or quantum dot case. These regions are accumulated around the InAs-rich region. One may speculate that the effect originates either from perculiarities of growth (switching on or off of the nitrogen plasma source prior to the InGaAsN growth, or after it) or form the self-organized strain compensation effect related to the phase separation of InAs and GaN phases. In the small-composition case the N-rich regions are formed near the top and bottom interfaces. We note that in-plane compositional nonuniformities (2% modulation of the lattice parameter in vertical direction) are revealed in the InGaAsN layers with low indium content and nominally lower average lattice mismatch with the substrate, as compared to the stable InGaAs quantum wells with similar indium composition. This indicates the nitrogen-activated phase separation process occurs despite of the small average lattice mismatch with the substrate. In the group of the samples, emitting at and beyond 1.1 μm at 300 K, in addition to compositional modulations, a very pronounced modulation of the layer thickness was observed [2, 3]. The group includes samples with composition of $x = 0.3$ and composition $x = 0.25$ and $y \sim 75$ W. A HREM image a the map of local interplane distance are demonstrated in Fig. 1(c),(d). One can see that the effective height of the contrast Is greatly increased as compared to the nominal well width. This is typical for self-organized InGaAs quantum dot structures. A typical size of the modulation is given in Table 1 and is equal about 30 nm. Processed maps of local interplane distance indicate also regions with a small value of lattice parameter ($\delta\, a_{InGaAsN}/a_{GaAs} \sim -0.03$). This again indicates nitrogen decoration. The nitrogen-rich region decorates In-rich quantum dot forming a curved shell-like arrangement. Increase in the nitrogen content for the same indium concentration causes stronger effect of phase separation. Plan view TEM image and its Fourier transformation of an indium-rich InGaAsN insertion are given in Fig. 2. One can see that the structure is composed of nanodomains with a typical size about 20–30 nm. The results agree well with the TEM data in cross-section geometry. The density of the nanodomains is about p~10^{10} cm^{-3}. Fourier transform images contain ordered spots indicating partial ordering of the domain size and their orientation.

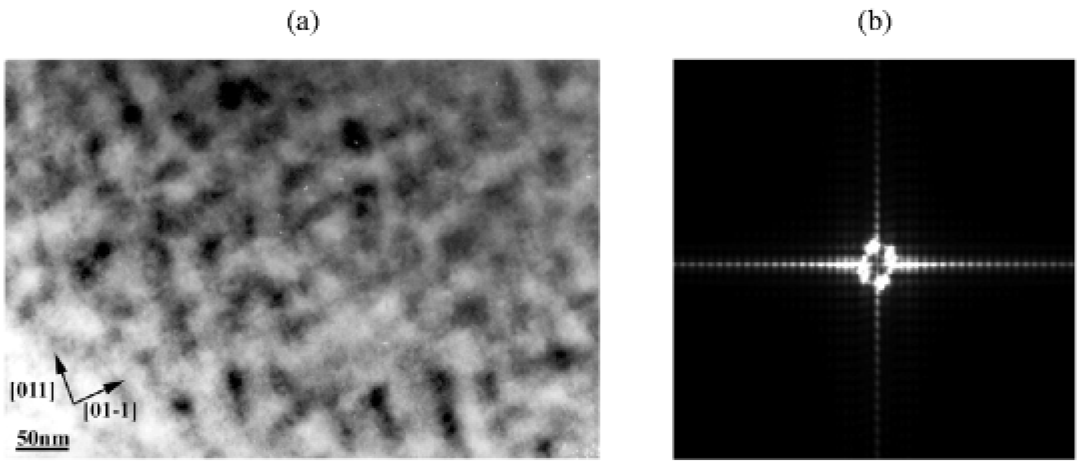

Fig 2. Plan view TEM image of $In_{0.25}Ga_{0.75}As_{0.99}N_{0.01}$/GaAs (a) structure and its Fourier transformation image (b).

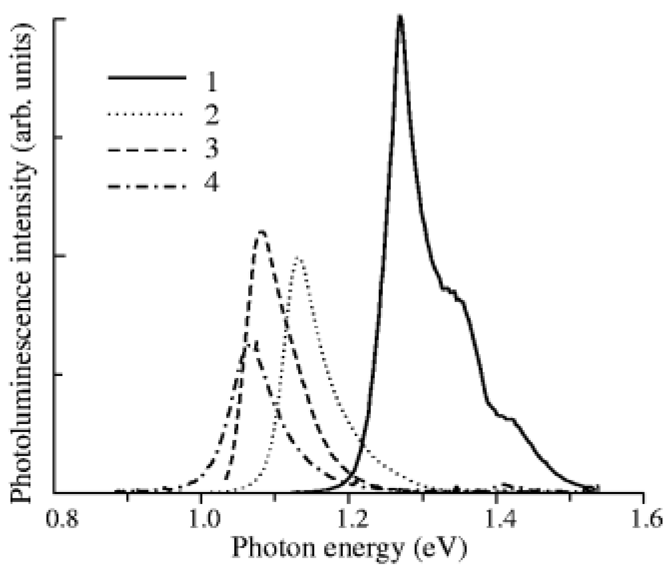

Fig 3. PL spectra of InGaAsN/GaAs structures. 1—x = 0.25, y~ 0 W, 2—x = 0.25, y~ 75 W, 3—x = 0.30, y~160 W, 4—x = 0.4, y~ 75 W.

PL spectra of the structures studied are given in Fig. 3. The spectra contain an InGaAsN-related line at 1.0–1.2 eV. The width of the PL peak of samples with the interface modulation (80–90 meV) is increased as compared to that in layer-like samples, as expected from the nanodomain formation [11].

Conclusions

InGaAsN/GaAs insertions grown by MBE growth have been investigated. In addition to the transition to laterally-corrugated growth we found an effect of nitroden decoration of the In-rich regions.

Acknowledgments

Authors are greatly Dr. I. Haehnert and D. Lucht for help to TEM specimen preparation. Parts of this work are supported by NATO SfP programme, CRDF and the Russian Foundation for Basic Research.

References

1. G. Steine, H. Riechert and A. Yu. Egorov, *Electr. Lett.* **37**, 93 (2001).
2. B. V. Volovik, A. R. Kovsh, W. Passenberg, H. Kuenzel, N. N. Ledentsov and V. M. Ustinov, *Tech. Phys. Lett.* **26**, 443 (2000).
3. B. V. Volovik, A. R. Kovsh, W. Passenberg, H. Kuenzel, N. Grote, N. A. Cherkashin, Yu. G. Musikhin, N. N. Ledentsov, D. Bimberg and V. M. Ustinov, *Semicond. Sci. Techn.* **16**, (2001), in print.
4. T. Miyamoto, K. Takeuchi, T. Kageyama, F. Koyama and K. Iga, *J. Cryst. Growth* **197**, 67 (1999).
5. S. Francoeur, G. Sivaraman, Y. Qiu, S. Nikishin and H. Temkin, *Appl. Phys. Lett.* **72**, 1857 (1998).
6. A. Yu. Egorov, A. E. Zhukov, A. R. Kovsh, V. M. Ustinov, V. V. Mamutin, S. V. Ivanov, V. N. Zhmerik, A. F. Tsatsul'nikov, D. A. Bedarev and P. S. Kop'ev, *Tech. Phys. Lett.* **24**, 942 (1998).
7. S. R. Kurtz, A. A. Alleman, E. D. Jones, J. M. Gee, J. Banas, *Appl. Phys. Lett.* **74**, 729 (1999).
8. Z. Pan, T. Miyamoto, D. Schlenker, S. Sato, F. Koyama, Kiga, *J. Appl. Phys.* **84**, 6409 (1998).
9. S. Sato and S. Satoh, *J. Cryst. Growth* **192**, 381 (1998).
10. I. P. Soshnikov, O. M. Gorbenko, A. O. Golubok and N. N. Ledentsov, *Semiconductors* **35**, 347 (2001) .
11. D. Bimberg M. Grundmann and N. N. Ledentsov, *Quantum Dot Heterostructures*, J. Wiley, 1999.
